

A Dynamic Open Framework Exhibiting Guest- and/or Temperature-Induced Bicycle-Pedal Motion in Single-Crystal to Single-Crystal Transformation

Manish K. Sharma and Parimal K. Bharadwaj*

Department of Chemistry, Indian Institute of Technology Kanpur, 208016, India

Received November 18, 2010

A ligand bis(4-imidazol-1-yl-phenyl)diazene (azim) incorporating an azo moiety at the center and two imidazole groups at the terminals forms two coordination polymers $\{[\text{Co}(\text{azim})_2(\text{DMF})_2] \cdot (\text{ClO}_4)_2 \cdot 2\text{DMF}\}_n$ (**1**) and $\{[\text{Cd}(\text{azim})_2(\text{DMF})_2] \cdot (\text{ClO}_4)_2 \cdot 2\text{DMF}\}_n$ (**2**) (DMF = *N,N*-dimethylformamide) at room temperature. Both **1** and **2** are isostructural with rhombic two-dimensional sheets stacking in ABAB... fashion resulting in large voids that contain DMF and ClO_4^- as guests. In **1**, the azo groups and phenyl rings are disordered over two positions and as in usual cases, the pedal motion cannot be discerned. Upon heating, **1** turns amorphous. In the case of **2**, however, heat treatment does not lead to loss of crystallinity. Thus, when a crystal of **2** (mother crystal) is heated slowly, it causes substantial movement or escape of both metal-bound and lattice DMF besides movement of ClO_4^- anions to give daughter crystals **2a**, **2b**, and **2c** without losing crystallinity (single-crystal to single-crystal (SC–SC) transformation). Most interestingly, the X-ray structures of **2** and its daughter products reveal stepwise reversible bicycle-pedal or crankshaft motion of the azo group. When a crystal of **2c** is kept in DMF for 10 h, crystal **2'** is formed whose structure is similar to that of **2** with slight changes in the bond distances and angles. Also, crystals of **2** are converted to **3** and **4** upon being kept in acetone or DEF (DEF = *N,N*-diethylformamide), respectively, for 10 h at ambient temperature in SC–SC transformation. In **3**, each lattice DMF molecule is replaced by an acetone molecule, leaving the two coordinated DMF molecules intact. However, in **4**, all lattice and coordinated DMF molecules are replaced by equal number of DEF molecules. Both in **3** and **4**, the azo moieties show bicycle-pedal motion. Thus, bicycle-pedal motion that normally cannot be observed is shown here to be triggered by heat as well as guest molecules in SC–SC fashion.

Introduction

In recent years, studies of coordination polymers have made a paradigm shift with the introduction of flexible and dynamic coordination polymers with structural¹ and functional² responses to guest sorption and other external stimuli. In such systems, dynamic behavior arises from the cooperative action of organic and inorganic moieties^{3,4} while the nature of flexibility depends mainly on the characteristics of the organic ligands used to build the frameworks. When the ligand contains mobile parts (for example, groups that undergo rotation or liberation), dynamic motion may occur inside the

framework in the solid state. Such motions in crystalline solids in response to outside stimuli such as light, heat, etc. are particularly intriguing. If the crystallinity of the compound is maintained, it is possible to observe the effects of molecular motions in terms of changes in the relative positions of the atoms via X-ray crystallography.

Molecular motions in crystalline solids have received attention in recent years due to their potential uses in fabricating nanoscale devices. Particularly, one of the most interesting phenomena is the bicycle-pedal or crankshaft motion. The pedal motion triggers conformational interconversion that results in disordered crystal structures if the conformers

*To whom correspondence should be addressed. E-mail: pkb@iitk.ac.in.

(1) (a) Kitagawa, S.; Kitaura, R.; Noro, S. *Angew. Chem., Int. Ed.* **2004**, *43*, 2334–2375. (b) Férey, G. *Chem. Soc. Rev.* **2008**, *37*, 191–214. (c) Batten, S. R.; Robson, R. *Angew. Chem., Int. Ed.* **1998**, *37*, 1460–1494. (d) Eddaoudi, M.; Moler, D. B.; Li, H. L.; Chen, B. L.; Reineke, T. M.; O'Keeffe, M.; Yaghi, O. M. *Acc. Chem. Res.* **2001**, *34*, 319–330. (e) Moulton, B.; Zaworotko, M. J. *Chem. Rev.* **2001**, *101*, 1629–1658. (f) Wang, Z.; Cohen, S. M. *Chem. Soc. Rev.* **2009**, *38*, 1315–1329. (g) Xiang, S.; Zhou, W.; Zhang, Z.; Green, M. A.; Liu, Y.; Chen, B. *Angew. Chem., Int. Ed.* **2010**, *49*, 4615–4618. (h) Farha, O. K.; Bae, Y. -S.; Hauser, B. G.; Spokoyny, A. M.; Snurr, R. Q.; Mirkin, C. A.; Hupp, J. T. *Chem. Commun.* **2010**, 1056–1058. (i) Kuznicki, S. M.; Bell, V. A.; Nair, S.; Hillhouse, H. W.; Jacobinas, R. M.; Braunbarth, C. M.; Toby, B. H.; Tspatsis, M. *Nature* **2001**, *412*, 720–724. (j) Halder, G. J.; Kepert, C. J. *J. Am. Chem. Soc.* **2005**, *127*, 7891–7900.

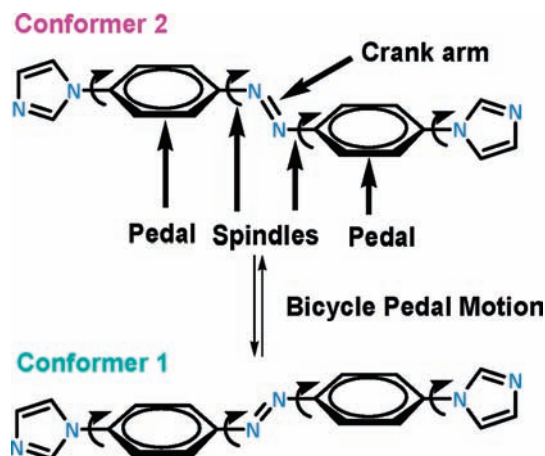
(2) (a) Chae, H. K.; Siberio-Perez, D. Y.; Kim, J. H.; Go, Y. -B.; Eddaoudi, M.; Matzger, A. J.; O'Keeffe, M.; Yaghi, O. M. *Nature* **2004**, *427*, 523–527. (b) Atwood, J. L.; Barbour, L. J.; Jerga, A.; Schottel, B. L. *Science* **2002**, *298*, 1000–1002. (c) Yaghi, O. M.; Li, G. M.; Li, H. L. *Nature* **1995**, *378*, 703–706. (d) Hang, J. W.; Hill, C. L. *J. Am. Chem. Soc.* **2007**, *129*, 15094–15095. (e) Wu, C. D.; Lin, W. *Angew. Chem., Int. Ed.* **2007**, *46*, 1075–1078. (f) Alaerts, L.; Seguin, E.; Poelman, H.; Thibault-Starzyk, F.; Jacobs, P. A.; De Vos, D. E. *Chem.—Eur. J.* **2006**, *12*, 7353–7363. (g) Klein, N.; Senkowska, I.; Gedrich, K.; Stoeck, U.; Henschel, A.; Mueller, U.; Kaskel, S. *Angew. Chem., Int. Ed.* **2009**, *48*, 9954–9957. (h) Maspocho, D.; Ruiz-Molina, D.; Wurst, K.; Domingo, N.; Cavallini, N.; Biscarini, F.; Tejada, J.; Rovira, C.; Veciana, J. *Nat. Mater.* **2003**, *2*, 190–195. (i) Beauvais, L. G.; Shores, M. P.; Long, J. R. *J. Am. Chem. Soc.* **2000**, *122*, 2763–2772.

have low energy barrier. However, if the energy barrier is high, the pedal motion does not show any disordering in the crystal structure due to insignificant population of the minor conformer.⁵ This motion has not been widely acknowledged because it is often difficult to detect and, therefore, easy to overlook. However, once we recognize the prevalence of the pedal motion, many dynamic phenomena can be interpreted on the basis of this motion, irrespective of its detection.

The pedal motion has been shown to be active in several organic crystals. It has been studied in crystals of bis-(triarylmethyl)peroxide,⁶ polyenes,⁷ and azobenzene.⁸ Its role in [2 + 2] photodimerization of alkene derivatives has been reported recently.⁹ The isomerization in butadienes through the pedal motion is reminiscent of the photoisomerization in the visual pigment rhodopsin.¹⁰ A recently proposed interpretation of the photocycle of photoactive yellow protein (PYP) also emphasized the potential importance of the pedal motion in proteins.¹¹ MacGillivray and co-workers have reported a rare example of the racklike movement of alkyl chains that coupled with pinionlike 180° rotation of olefins in a single crystal.¹²

Herein, we report the synthesis of two two-dimensional (2D) coordination polymers, $\{[\text{Co}(\text{azim})_2(\text{DMF})_2] \cdot (\text{ClO}_4)_2 \cdot 2\text{DMF}\}_n$ (**1**) and $\{[\text{Cd}(\text{azim})_2(\text{DMF})_2] \cdot (\text{ClO}_4)_2 \cdot 2\text{DMF}\}_n$ (**2**) prepared at room temperature by reacting $\text{M}(\text{ClO}_4)_2$ ($\text{M}(\text{II}) = \text{Co}(\text{II})$ and $\text{Cd}(\text{II})$) with the ligand, bis(4-imidazol-1-yl-phenyl)diazene (azim). The ligand is designed with an azo moiety in the middle for possible bicycle-pedal motion. Here, the two phenyl rings are attached to the central $\text{N}=\text{N}$ moiety. The relationships among these parts are similar to those of bicycle pedals (phenyl rings), crank arms ($\text{N}=\text{N}$ bond), and spindles ($\text{N}-\text{Ph}$ bonds) (Scheme 1). The azo bonds and phenyl rings are disordered in the solid-state structure of **1**, over two positions due to crankshaft motion. Interestingly, this disorder is not observed in **2**. Therefore, we have chosen polymer **2** to study heat-/guest-dependent bicycle-pedal motion. Ad-

Scheme 1. Schematic Representation of Pedal Motion in the Diphenyldiazene Moieties in Ligand (azim)



ditionally, there has been comparatively little attention directed toward reversible, concerted ligand substitution at metal sites in PCPs in single-crystal to single-crystal (SC-SC) fashion, leading to expression of new functionality.¹³ In compound **2**, the guest molecules including the counteranions make significant movement, and the counteranions eventually occupy vacant coordination sites on the metal, keeping crystallinity intact throughout.

Results and Discussion

Compounds **1** and **2**, once isolated, are found to be air-stable and slightly soluble in DMF and DMSO, but insoluble in other common organic solvents or water. Single-crystal X-ray determination at 100 K reveals that both **1** and **2** are isostructural and the asymmetric unit of each polymer contains one $\text{M}(\text{II})$ ion (half occupancy), two halves of the ligand, two DMF molecules, and one ClO_4^- anion. Each metal ion is distorted octahedral with equatorial ligation by imidazole N of four different ligand units and axial ligation by two DMF molecules (Figure 1) with $\text{M}-\text{N}$ and $\text{M}-\text{O}$ bond distances^{14,15} within normal ranges. The ligands bridge metal ions to form a 2D rhombus-grid structure. Both phenyl rings of the ligand are nearly coplanar, while imidazole rings are twisted significantly with respect to the phenyl rings. Each grid (M_4L_4) shows the diagonal $\text{M} \cdots \text{M}$ distances of 33.922 and 20.151 Å in **1** and 34.759 and 20.275 Å in **2** (Table 1, Figure 2). These 2D layers are stacked in *ABAB*... fashion.¹⁶ Lattice DMF molecules and ClO_4^- anions occupy the void spaces in the grid. In case of **1**, diphenyldiazene moiety of the ligand **A** and **C** in the M_4L_4 macrocyclic unit are disordered over two positions because of the pedal motion and both conformers of the ligand are distributed in the crystal (Figure 3a). On the other hand, no such disorder is observed in case of **2** (Figure 3b). Thermal analyses of **1** and **2** show weight losses of ~27 and ~23.4% respectively, in the temperature range 70–150 °C, that correspond to loss of both lattice and coordinated DMF molecules. The desolvated frameworks are stable up to ~340 °C.¹⁶ IR spectra of **1** and **2** show a C–H stretching vibration at ~2930 cm^{-1} and a C=O stretching

(3) (a) Seo, J.; Matsuda, R.; Sakamoto, H.; Bonneau, C.; Kitagawa, S. *J. Am. Chem. Soc.* **2009**, *131*, 12792–12800. (b) Lee, Y. E.; Jang, S. Y.; Suh, M. P. *J. Am. Chem. Soc.* **2005**, *127*, 6374–638.

(4) (a) Uemura, K.; Kitagawa, S.; Fukui, K.; Saito, K. *J. Am. Chem. Soc.* **2004**, *126*, 3817–3828. (b) Matsuda, R.; Kitaura, R.; Kitagawa, S.; Kubota, Y.; Kobayashi, T. C.; Horike, S.; Takata, M. *J. Am. Chem. Soc.* **2004**, *126*, 14063–14070. (c) Kitaura, R.; Seki, K.; Akiyama, G.; Kitagawa, S. *Angew. Chem., Int. Ed.* **2003**, *42*, 428–431.

(5) Harada, J.; Ogawa, K. *Chem. Soc. Rev.* **2009**, *38*, 2244–2252.

(6) Khuong, T. -A. V.; Zepeda, G.; Sanrume, C. N.; Dang, H.; Bartberger, M. D.; Houk, K. N.; Garcia-Garibay, M. A. *J. Am. Chem. Soc.* **2004**, *126*, 14778–14786.

(7) (a) Harada, J.; Ogawa, K. *J. Am. Chem. Soc.* **2004**, *126*, 3539–3544. (b) Harada, J.; Harakawa, M.; Ogawa, K. *CrystEngComm* **2008**, 1777–1781. (c) Galli, S.; Mercandelli, P.; Sironi, A. *J. Am. Chem. Soc.* **1999**, *121*, 3767–3772.

(8) (a) Harada, J.; Ogawa, K.; Tomoda, S. *Acta Crystallogr., Sect. B* **1997**, *53*, 662–672. (b) Harada, J.; Ogawa, K. *J. Am. Chem. Soc.* **2001**, *123*, 10884–10888.

(9) (a) Bhogala, B. R.; Captain, B.; Parthasarathy, A.; Ramamurthy, V. *J. Am. Chem. Soc.* **2010**, *132*, 13434–13442. (b) Peedikakkal, A. M. P.; Vittal, J. J. *Chem.—Eur. J.* **2008**, *14*, 5329–5334. (c) Chu, Q.; Swenson, D. C.; MacGillivray, L. R. *Angew. Chem., Int. Ed.* **2005**, *44*, 3569–3572.

(10) (a) Gascón, J. A.; Sproviero, E. M.; Batista, V. S. *Acc. Chem. Res.* **2006**, *39*, 184–193. (b) Schapiro, I.; Weingart, O.; Buss, V. *J. Am. Chem. Soc.* **2009**, *131*, 16–17.

(11) Liu, R. S. H.; Hammond, G. S. *Acc. Chem. Res.* **2005**, *38*, 396–403. (12) Sokolov, A. N.; Swenson, D. C.; MacGillivray, L. R. *Proc. Natl. Acad. Sci. U.S.A.* **2008**, *105*, 1794–1797.

(13) (a) Das, M. C.; Bharadwaj, P. K. *J. Am. Chem. Soc.* **2009**, *131*, 10942–10949. (b) Das, M. C.; Bharadwaj, P. K. *Chem.—Eur. J.* **2010**, *16*, 5070–5077. (c) Bradshaw, D.; Warren, J. E.; Rosseinsky, M. J. *Science* **2007**, *315*, 977–980. (d) Halder, G. J.; Keppert, C. J.; Moubaraki, B.; Murray, K. S.; Cashion, J. D. *Science* **2002**, *298*, 1762–1765.

(14) Neogi, S.; Sharma, M. K.; Das, M. C.; Bharadwaj, P. K. *Polyhedron* **2009**, *28*, 3923–3928.

(15) Lama, P.; Aijaz, A.; Sañudo, E. C.; Bharadwaj, P. K. *Cryst. Growth Des.* **2010**, *10*, 283–290.

(16) See Supporting Information.

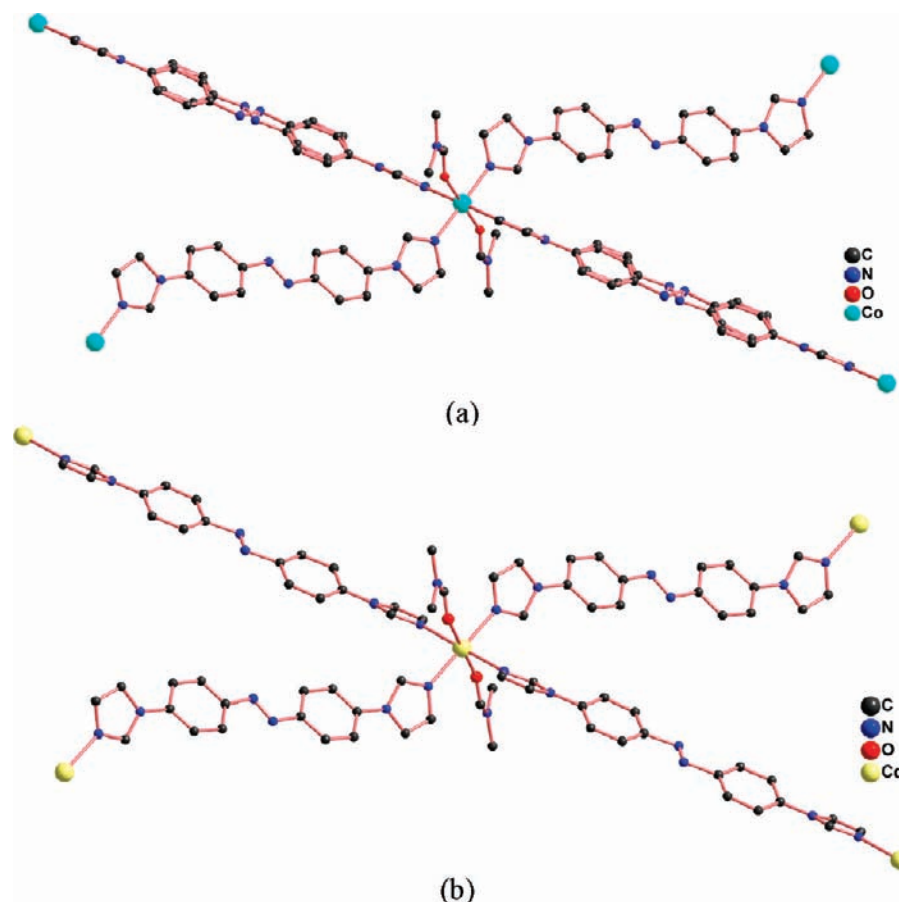


Figure 1. A perspective view of metal coordination environment in (a) **1**, (b) **2**.

Table 1. $M \cdots M$ Diagonal Distances Comparisons in M_4L_4 Macrocyclic Units of **1–4**, **2a**, **2b**, **2c** and **2'**

compounds	diagonal distance between $M1 \cdots M3$ (Å)	diagonal distance between $M2 \cdots M4$ (Å)
1	33.922	20.15
2	34.759	20.275
2a	34.557	20.004
2b	34.690	19.762
2c	36.328	16.301
3	34.724	20.495
4	34.216	21.581
2'	34.749	20.633

vibration of DMF at $\sim 1675 \text{ cm}^{-1}$, while a broad band centers around 1095 cm^{-1} due to ionic ClO_4^- anions.¹⁶

Heat-Induced SC–SC Transformation Studies. In order to investigate the pedal motion, a suitable crystal of **2** (mother crystal) is chosen and used throughout. On careful heating at 50°C for 2 h under vacuum, crystal **2** forms the partially desolvated compound, $\{[\text{Cd}(\text{azim})_2(\text{DMF})_2] \cdot (\text{ClO}_4)_2 \cdot (1.33\text{DMF})\}_n$ (**2a**) without losing crystallinity. Each Cd(II) ion remains octahedral with coordination similar to that in **2**. While Cd–N bond distances remain almost the same as in **2**, the Cd–O (DMF) bond distances become longer.¹⁶ The rhombic grid framework is shortened with the diagonal $M \cdots M$ distances of 34.557 and 20.004 Å (Table 1, Figure 2). Also, one of the ClO_4^- anions moves toward the nearest Cd(II) from 5.997 Å to 5.771 Å while the other moves away from 5.997 to 6.639 Å (the distance refers to Cd \cdots Cl). Most interestingly, the diphenyldiazene moiety of the ligand **A** (Figure 4) in the

M_4L_4 macrocyclic unit shows bicycle-pedal or crankshaft motion. Now, the phenyl rings are no longer coplanar but are twisted, forming a dihedral angle of 24.18° . The imidazole rings also move away from coplanarity and make a dihedral angle of $\sim 15^\circ$ with respect to each other. The two phenyl rings in ligand **B** also move out of coplanarity to a dihedral angle of 26.83° . The overall structure of **2a** shows two consecutive rows of channels filled with DMF followed by one row of empty channels.¹⁶ To the best of our knowledge, this is the first example of guest dependent pedal motion in SC–SC fashion observed in metal complexes or coordination polymers.

Further heating of the crystal **2a** at 70°C for 2 h under vacuum, affords $\{[\text{Cd}(\text{azim})_2(\text{DMF})_2] \cdot (\text{ClO}_4)_2 \cdot (\text{DMF})\}_n$ (**2b**) still maintaining crystallinity. As before, each Cd(II) center exhibits distorted octahedral geometry with the same coordination mode as in **2** and **2a**. Neither the metal-bound DMF nor the ClO_4^- anions make any significant movement compared to the situation in **2a**. Here, partial expulsion of lattice DMF takes place although the 2D rhombus grid framework is maintained albeit with slightly different diagonal $M \cdots M$ distances of 34.693 and 19.762 Å (Table 1 and Figure 2). Now, the ligand **C** also undergoes bicycle-pedal motion (Figure 4) and all phenyl rings of the four azim ligands (**A–D**) in the M_4L_4 unit are twisted away from coplanarity. The overall structure of **2b** shows the rhombic channels in the grid are empty at alternate rows.¹⁶

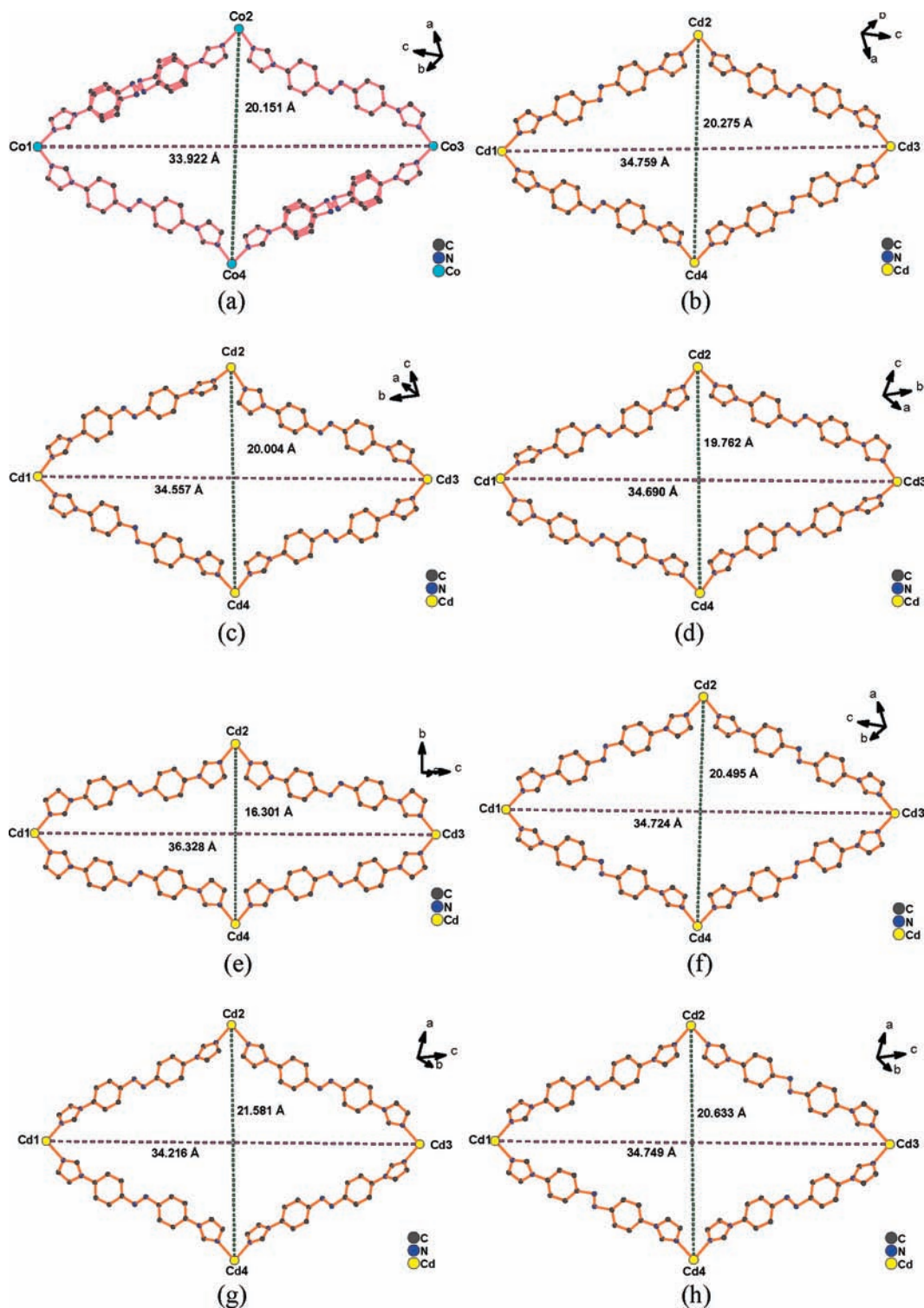


Figure 2. Crystal structure showing the $M \cdots M$ diagonal distances in (a) **1**, (b) **2**, (c) **2a**, (d) **2b**, (e) **2c**, (f) **3**, (g) **4**, (h) **2'**.

Crystal **2b** on further heating at 120 °C for another 2 h gives completely desolvated compound $\{[\text{Cd}(\text{azim})_2(\text{ClO}_4)_2]\}_n$ (**2c**). Although this crystal is of poor quality and several cracks can be seen, still an approximate single crystal X-ray structure is obtained. The framework is maintained here with significantly different $M \cdots M$ diagonal distances of 36.328 and 16.301 Å (Table 1, Figure 2). Here, all DMF molecules are lost and the ClO_4^- anions move further and occupy both the axial positions on the metal.¹⁶

The ClO_4^- anions become highly disordered. Orientations of the azo group remain unaltered with respect to the situation in **2b**. In the IR spectrum of **2c**, the bands at 2930 and 1670 cm^{-1} disappear, suggesting the absence of DMF molecules in the framework. The broad band at $\sim 1100 \text{ cm}^{-1}$ corresponding to ionic ClO_4^- splits into two bands due to coordination of ClO_4^- anions to Cd(II) centers.¹⁷

Guest-Induced SC–SC Transformation Studies. When crystal **2c** is kept in DMF, it turns shiny and transparent

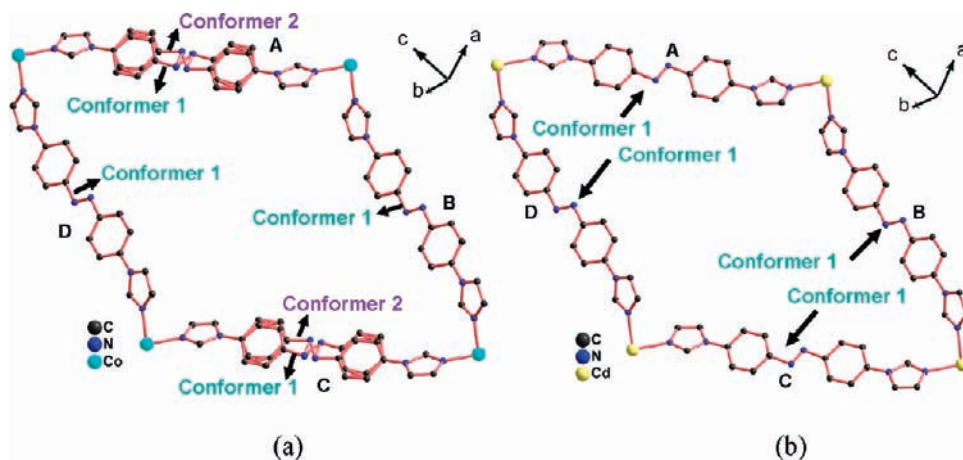


Figure 3. View of M_4L_4 rhombus grid of (a) **1** showing disordered diphenyldiazeno moieties of azim (units A and C) due to dynamic pedal motion, (b) **2** (no disorder is observed).

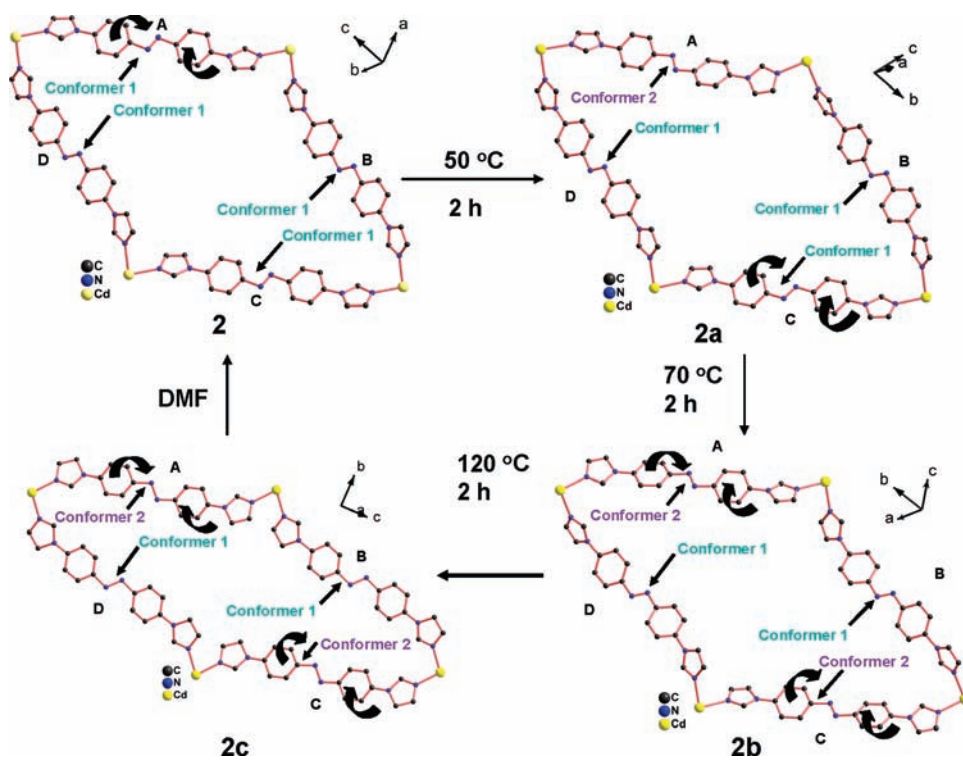


Figure 4. Schematic representation of reversible SC–SC pedal motion and twisting of phenyl rings in compound **2** after guest removal by heating (guest molecules are removed for clarity).

(we call it **2'**). X-ray structural studies on **2'** reveal that the structure is quite similar to that of **2** with slight differences in the bond distances and bond angles involving the metal ion. This also shows removal of DMF molecules from the framework, and its readmission occurs in SC–SC fashion. Also, the pedal motion of ligands A and C in **2'** change to the initial position observed in **2**, indicating this motion to be reversible in nature (Figure 4). To probe the effect of different solvents on the pedal motion, another crystal of compound **2** is kept in acetone for 10 h at RT that affords crystal **3** as $\{[\text{Cd}(\text{azim})_2(\text{DMF})_2] \cdot (\text{ClO}_4)_2 \cdot 2\text{acetone}\}_n$ without losing crystallinity. Its structure reveals that the M_4L_4 macrocyclic framework remains the

same as that in **2**. Each Cd(II) ion is octahedral with coordination similar to that in **2**. However, each lattice DMF molecule is replaced by an acetone molecule. Most interestingly, diphenyldiazeno moieties of the ligands **B** and **D** in the M_4L_4 macrocyclic unit have undergone pedal motion (Figures 5 and 6). When crystal **3** is kept in DMF for 10 h, the crystal is found to be transformed to the original **2** with slight differences in the bond distances and bond angles involving the metal ion. The diagonal $M \cdots M$ distances are almost restored (34.749 and 20.633 Å compared to 34.759 and 20.275 Å in the original (**2**), and the conformations of the diphenyldiazeno moieties are also restored to the original conformations (as in **2**).

When crystal **2** is kept in DEF for 10 h at RT, it gives crystal **4** without losing crystallinity. Here, each DMF

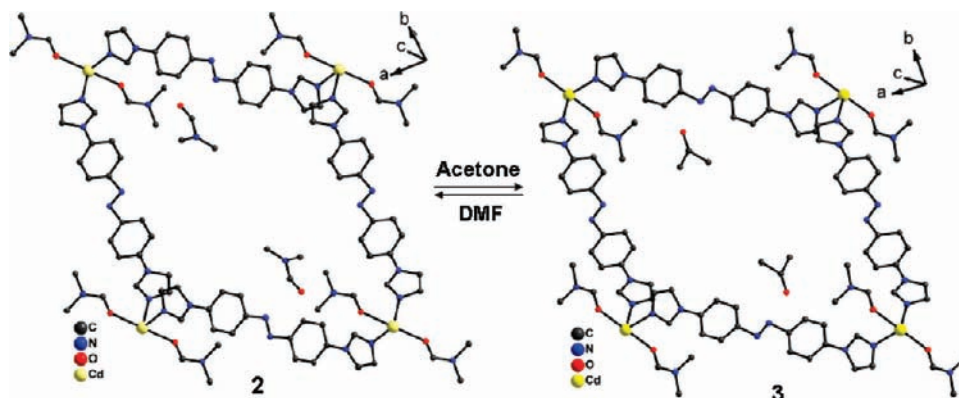


Figure 5. Schematic representation of reversible SC–SC acetone/DMF exchange in compound **2** (H atoms are removed for clarity).

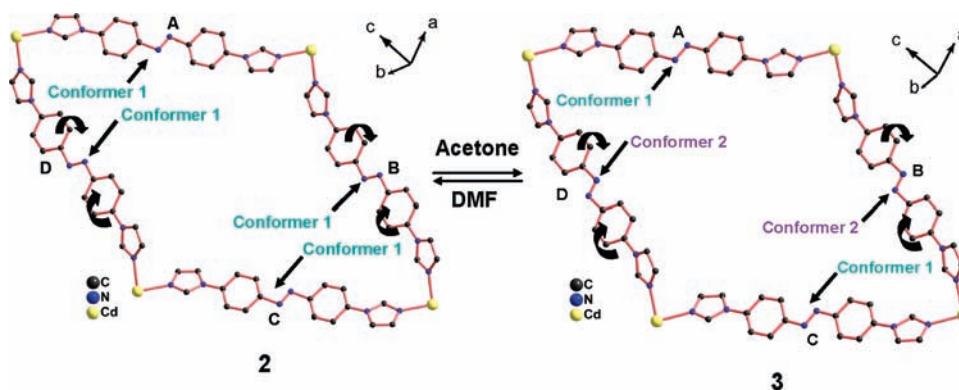


Figure 6. Schematic representation of reversible SC–SC pedal motion in compound **2** after acetone/DMF exchange (guest molecules are removed for clarity).

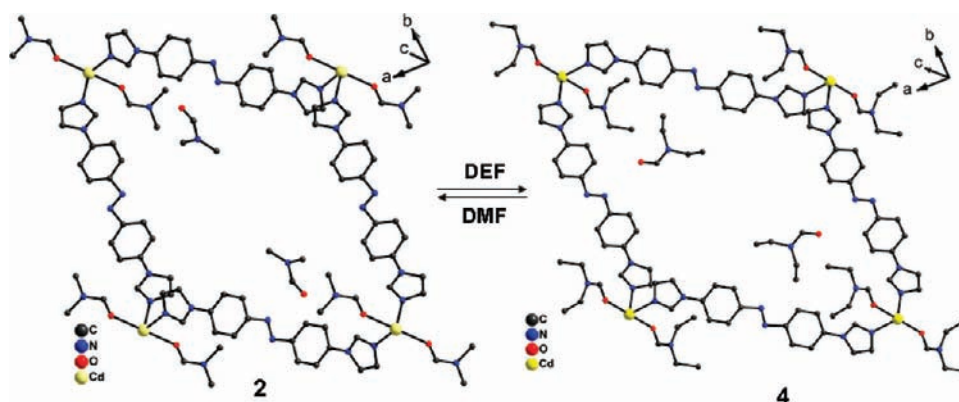


Figure 7. Schematic representation of reversible SC–SC DEF/DMF exchange in compound **2** (H atoms are removed for clarity).

molecule (coordinated or lattice) is replaced by a DEF molecule retaining the framework with the diagonal $M \cdots M$ distances of 34.724 and 20.495 Å. It is found that diphenyldiazene moieties of ligands A and C in the M_4L_4 macrocycle have undergone pedal motion (Figures 7 and 8). To study whether these dynamic pedal motions are reversible, the crystal **4** is kept in DMF at RT to get crystal **2** as above. Thus, these pedal motions are completely reversible in nature. During the substitution reactions, transparency of the single crystal is retained. The possibility of dissolution of the mother crystal (**2**) in the successive liquids followed by crystallization or renucleation at the surface and growth of the new phase is excluded as shown by the

photographs taken (Figure 9) of the mother crystal (**2**) and its transformations to **2a**, **2b**, **2c**, **2'**, **3**, or **4** which show no change in size, morphology, color, and transparency.

Conclusion

In conclusion, we have shown here that the ligand, bis(4-imidazol-1-yl-phenyl)diazene(L) having two imidazole units at each end, forms non-interpenetrated rhombus grid networks that stack in *ABAB*... fashion, with two DMF molecules and two ClO_4^- anions occupying the void space. The coordination polymer **2** shows guest- and heat-induced stepwise dynamic bicycle-pedal or crankshaft motion in the ligand moieties without losing crystallinity. To the best of



Figure 8. Schematic representation of reversible SC–SC pedal motion in compound **2** after DEF/DMF exchange (guest molecules are removed for clarity).

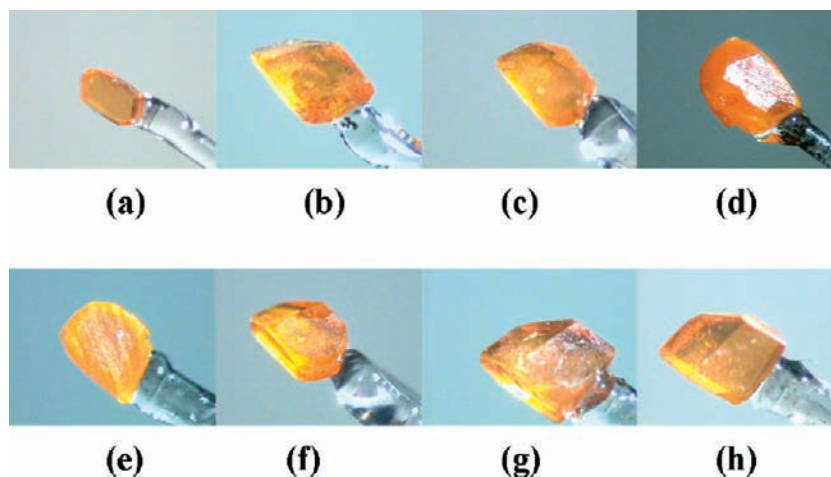


Figure 9. Photographs of single crystals of (a) **1**, (b) **2**, (c) **2a**, (d) **2b**, (e) **2c**, (f) **2'**, (g) **3**, and (h) **4**.

our knowledge, this is the first example of guest-/heat-dependent reversible pedal motion observed in a coordination polymer.

Experimental Section

Materials. The metal salts were obtained from Aldrich and used as received. All other chemicals were procured from Aldrich and S.D. Fine Chemicals, India. All solvents were purified prior to use.

Caution! Perchlorate salts are explosive (especially if they are dry) and should be handled with extreme caution. We had not encountered any problem during this work. In order to know the thermal stability of complexes (**1–5** and **1'**), we had heated 100 mg of each sample separately at 200 °C (heating rate 5 °C/min.) for 6 h, and we did not face any problem. All the complexes described herein are stable in air, moisture, and all the solvents used. To minimize hazards associated with perchlorate complexes the following precautions should be taken: (i) keep reaction scales to < 100 mg, (ii) do not heat the complexes above 200 °C, not exceeding the heating rate above 5 °C/min, and (iii) carry out all reactions in an efficient fume hood!

Preparation of Ligand. The ligand bis(4-imidazol-1-yl-phenyl)diazene was prepared in two steps as described below.

(i) **Preparation of 1-(4-Nitrophenyl)-1H-imidazole.** A mixture of imidazole (2.1 g, 31.18 mmol) and anhydrous K₂CO₃ (5.8 g, 42.52 mmol) in DMF was heated for 30 min with vigorous stirring. After that, 4-fluoronitrobenzene (4 g, 28.34 mmol) was added over a period of 15 min. The mixture was refluxed for 24 h, cooled to RT, and then added to ice–water. On standing, a yellow-colored precipitate was formed which was collected by filtration, washed

with ice-cold water, and dried in air to get the pure compound (yield 85%). ¹H NMR (CDCl₃, 400 MHz): 7.21(s, 1H; H_{Ar}), 7.32(s, 1H; H_{Ar}), 7.52(d, *J* = 9.28 Hz, 2H; H_{Ar}), 7.94(s, 1H; H_{Ar}), 8.31(d, *J* = 9.28 Hz, 2H; H_{Ar}); Anal. Calcd for C₉H₇N₃O₂: C, 57.14; H, 3.73; N, 22.21%. Found: C, 57.18; H, 3.71; N, 22.24%.

(ii) **Preparation of Bis(4-imidazol-1-yl-phenyl)diazene (L).** A suspension of 1-(4-nitrophenyl)-1H-imidazole (5 g, 26.45 mmol) in 2-propanol was heated to reflux to obtain a clear solution. Then aq NaOH (12 g in 30 mL H₂O) and Zn powder (30 g) were added to the mixture. It was then refluxed for 24 h and allowed to cool to RT, and all insoluble materials present were removed by filtration. Upon removal of the solvent under reduced pressure, the product was extracted with chloroform. The organic layer was washed several times with water, dried over anhydrous Na₂SO₄, and finally evaporated under reduced pressure to obtain a bright-orange solid which was recrystallized from hexane/chloroform to get the pure compound (yield 70%). ¹H NMR (CDCl₃, 400 MHz): 7.00 (s, 1H; H_{Ar}), 7.31 (s, 1H; H_{Ar}), 7.13 (d, *J* = 8.56 Hz, 2H; H_{Ar}), 7.56 (s, 1H; H_{Ar}), 7.48 (d, *J* = 8.8 Hz, 2H; H_{Ar}); IR (cm⁻¹, KBr pellet): 3103, 1599, 1515, 1305; ESI-MS: *m/z* [M]⁺ 315; calculated 314.65; Anal. Calcd for C₁₈H₁₄N₆: C, 68.78; H, 4.49; N, 26.79%. Found: C, 68.82; H, 4.54; N, 26.71%.

Preparation of {[Co(L)₂(DMF)₂](ClO₄)₂·(2DMF)}_n (1**).** A hot DMF solution (3 mL) of ligand **L** (50 mg, 0.16 mmol) was added to MeOH/H₂O mixed solution (1:1, 2 mL) of Co(ClO₄)₂·6H₂O (58 mg, 0.16 mmol). On slow evaporation of the filtrate at RT, red crystals were obtained in ~80% yield. Anal. Calcd for C₄₈H₅₆CoCl₂N₁₆O₁₂: C, 48.90; H, 4.79; N, 19.01%. Found: C, 48.92; H, 4.77; N, 19.03%.

Table 2. Crystal and Structure Refinement Data for 1, 2, 3, 4, and 2'

compound	1	2	3	4	2'
formula	C ₄₈ H ₅₆ CoCl ₂ N ₁₆ O ₁₂	C ₄₈ H ₅₆ CdCl ₂ N ₁₆ O ₁₂	C ₄₈ H ₅₄ CdCl ₂ N ₁₄ O ₁₂	C ₅₆ H ₇₂ CdCl ₂ N ₁₆ O ₁₂	C ₄₈ H ₅₆ CdCl ₂ N ₁₆ O ₁₂
formula weight	1178.92	1232.39	1202.35	1344.60	1232.38
temperature (K)	100	100	100	100	100
radiation	Mo K α	Mo K α	Mo K α	Mo K α	Mo K α
wavelength (Å)	0.71069	0.71069	0.71069	0.71069	0.71069
crystal system	triclinic	triclinic	triclinic	triclinic	triclinic
space group	P1	P1	P1	P1	P1
<i>a</i> , Å	9.251(4)	9.233(5)	9.304(3)	10.203(5)	9.389(5)
<i>b</i> , Å	10.409(5)	10.375(6)	10.370(5)	10.415(5)	10.442(6)
<i>c</i> , Å	14.972(4)	15.393(4)	15.502(2)	15.118(5)	15.507(5)
α (deg)	76.483(3)	76.162(5)	77.703(6)	76.404(5)	77.828(4)
β (deg)	75.520(4)	75.294(3)	75.330(5)	77.217(5)	75.570(5)
γ (deg)	83.351(6)	84.377(5)	84.982(5)	82.000(5)	84.742(5)
<i>U</i> , Å ³	1354.7(9)	1383.7(12)	1412.8(8)	1516.3(12)	1438.0(12)
<i>Z</i>	1	1	1	1	1
ρ_{calc} g/cm ³	1.445	1.479	1.413	1.472	1.423
μ , mm ⁻¹	0.491	0.566	0.551	0.523	0.544
reflectns collected	613	634	618	698	634
<i>R</i> _{int}	0.0248	0.0223	0.0421	0.0249	0.0297
independent reflectns	4679	4806	4881	5215	5001
refinement method	full-matrix least-squares on <i>F</i> ²	full-matrix least-squares on <i>F</i> ²	full-matrix least-squares on <i>F</i> ²	full-matrix least-squares on <i>F</i> ²	full-matrix least-squares on <i>F</i> ²
GOF	1.117	1.051	1.070	1.123	1.161
final <i>R</i> indices [<i>I</i> > 2 σ (<i>I</i>)]	<i>R</i> ₁ = 0.0626 <i>wR</i> ₂ = 0.1658	<i>R</i> ₁ = 0.0603 <i>wR</i> ₂ = 0.1583	<i>R</i> ₁ = 0.0790 <i>wR</i> ₂ = 0.2033	<i>R</i> ₁ = 0.0630 <i>wR</i> ₂ = 0.1668	<i>R</i> ₁ = 0.0724 <i>wR</i> ₂ = 0.1840
<i>R</i> indices (all data)	<i>R</i> ₁ = 0.0769 <i>wR</i> ₂ = 0.1972	<i>R</i> ₁ = 0.0639 <i>wR</i> ₂ = 0.1618	<i>R</i> ₁ = 0.1040 <i>wR</i> ₂ = 0.2431	<i>R</i> ₁ = 0.0719 <i>wR</i> ₂ = 0.1901	<i>R</i> ₁ = 0.0828 <i>wR</i> ₂ = 0.2027

Table 3. Crystal and Structure Refinement Data for **2a**, **2b**, and **2c**

compound	2a	2b	2c
formula	C ₁₃₈ H ₁₅₄ Cd ₃ Cl ₆ N ₄₆ O ₃₄	C ₄₅ H ₄₉ CdCl ₂ N ₁₅ O ₁₁	C ₃₆ H ₂₈ CdCl ₂ N ₁₂ O ₈
formula weight	3550.97	1159.29	940.00
temperature (K)	100	100	100
radiation	Mo K α	Mo K α	Mo K α
wavelength (Å)	0.71069	0.71069	0.71069
crystal system	triclinic	triclinic	monoclinic
space group	$P\bar{1}$	$P\bar{1}$	$C2/m$
<i>a</i> , Å	10.449(5)	10.453(2)	14.436(6)
<i>b</i> , Å	15.150(3)	15.212(5)	16.301(3)
<i>c</i> , Å	26.857(2)	17.753(3)	16.996(4)
α (deg)	74.102(2)	72.53(3)	90.000
β (deg)	87.250(5)	84.76(2)	92.576(5)
γ (deg)	74.714(4)	74.64(3)	90.000
<i>U</i> , Å ³	3943(2)	2596.3(12)	3995(2)
<i>Z</i>	1	2	2
ρ_{calc} g/cm ³	1.495	1.483	0.781
μ , mm ⁻¹	0.591	0.596	0.374
<i>F</i> (000)	1822	1188	948
reflectns collected	27818	18273	10009
<i>R</i> _{int}	0.0523	0.0596	0.0888
independent reflectns	13726	9039	3599
refinement method	full-matrix least-squares on <i>F</i> ²	full-matrix least-squares on <i>F</i> ²	full-matrix least-squares on <i>F</i> ²
GOF	1.043	1.026	1.896
final <i>R</i> indices [<i>I</i> > 2 σ (<i>I</i>)]	<i>R</i> 1 = 0.0660 <i>wR</i> 2 = 0.1645	<i>R</i> 1 = 0.0846 <i>wR</i> 2 = 0.2245	<i>R</i> 1 = 0.1874 <i>wR</i> 2 = 0.4326
<i>R</i> indices (all data)	<i>R</i> 1 = 0.0937 <i>wR</i> 2 = 0.1972	<i>R</i> 1 = 0.1348 <i>wR</i> 2 = 0.2658	<i>R</i> 1 = 0.2009 <i>wR</i> 2 = 0.4550

Preparation of {[Cd(L)₂(DMF)₂](ClO₄)₂·(2DMF)}_{*n*} (2**).** A hot DMF solution (3 mL) of ligand **L** (50 mg, 0.16 mmol) was added to MeOH/H₂O mixed solution (1:1, 2 mL) of Cd(ClO₄)₂·*x*H₂O (49 mg, 0.16 mmol). On slow evaporation of the filtrate at RT, orange crystals were obtained in ~80% Yield. Anal. Calcd for C₄₈H₅₆CdCl₂N₁₆O₁₂: C, 46.78; H, 4.58; N, 18.19%. Found: C, 46.82; H, 4.60; N, 18.17%.

Preparation of {[Cd(L)₂(DMF)₂](ClO₄)₂·(1.33DMF)}_{*n*} (2a**).** Crystal of **2** was heated at 50 °C for 2 h under vacuum to obtain **2a**. Anal. Calcd for C₄₆H_{51.33}Cd₁Cl₂N_{15.33}O_{11.33}: C, 46.68; H, 4.37; N, 18.15%. Found: C, 46.70; H, 4.39; N, 18.12%.

Preparation of {[Cd(L)₂(DMF)₂](ClO₄)₂·(DMF)}_{*n*} (2b**).** Crystal of **2a** was heated at 70 °C for 2 h under vacuum to obtain **2b**. Anal. Calcd for C₄₅H₄₉CdCl₂N₁₅O₁₁: C, 46.62; H, 4.26; N, 18.12%. Found: C, 46.63; H, 4.24 N, 18.10%.

Preparation of {[Cd(L)₂(ClO₄)₂]}_{*n*} (2c**).** Crystal of **2b** was heated at 120 °C for 2 h under vacuum to obtain **2c**. Anal. Calcd for C₃₆H₂₈CdCl₂N₁₂O₈: C, 45.99 H, 3.00; N, 17.88%. Found: C, 46.01; H, 2.97; N, 17.91%.

Preparation of {[Cd(L)₂(DMF)₂](ClO₄)₂·(2acetone)}_{*n*} (3**).** Crystal of **2** on keeping in acetone at room temperature for 10 h affords **3**. Anal. Calcd for C₄₈H₅₄CdCl₂N₁₄O₁₂: C, 47.95; H, 4.53; N, 16.31%. Found: C, 47.92; H, 4.57; N, 16.29%.

Preparation of {[Cd(L)₂(DEF)₂](ClO₄)₂·(2DEF)}_{*n*} (4**).** A new crystal of **2** was immersed in DEF (0.1 mL) at room temperature for 10 h to obtain **4**. Anal. Calcd for C₅₆H₇₂CdCl₂N₁₆O₁₂: C, 50.02; H, 5.40; N, 16.67%. Found: C, 50.05; H, 5.39; N, 16.69%.

Preparation of {[Cd(L)₂(DMF)₂](ClO₄)₂·(2DMF)}_{*n*} (2'**).** Crystals of **2c**, **3**, and **4** were immersed in DMF separately at room temperature for 10 h to obtain **2'** in each case. Anal. Calcd for C₄₈H₅₆CdCl₂N₁₆O₁₂: C, 46.78; H, 4.58; N, 18.19%. Found: C, 46.79; H, 4.57; N, 18.16%.

Physical Measurements. Spectroscopic data were collected as follows: IR spectra (KBr disk, 400–4000 cm⁻¹) were recorded on a Perkin-Elmer model 1320 spectrometer. X-ray powder patterns (Cu K α radiation, 3 deg/min scan rate, 293 K) were acquired using a Philips PW100 diffractometer. Thermogravimetric analysis (TGA) (5 °C/min heating rate under a nitrogen atmosphere) was performed with a Mettler Toledo Star System. ¹H NMR spectra were recorded on a JEOL JNM-LA500 FT instrument (400 and 500 MHz) in CDCl₃ and DMSO-*d*₆ with TMS as the internal standard. Microanalysis data for the compounds were obtained from CDRI, Lucknow.

X-ray Structural Studies. Single-crystal X-ray data were collected at 100 K on a Bruker SMART APEX CCD diffractometer using graphite-monochromatized Mo K α radiation (λ , 0.71069 Å). The linear absorption coefficients, scattering factors for the atoms, and anomalous dispersion corrections were taken from the International Tables for X-ray Crystallography. The data integration and reduction were processed with SAINT¹⁸ software. An empirical absorption correction was applied to the collected reflections with SADABS¹⁹ using XPREP.²⁰ The structure was solved by the direct methods using SHELXTL²¹ and refined on *F*² by full-matrix least-squares techniques using the SHELXL-97 program package.²² Each of the C atoms of (C5–C9) of one benzene ring in the ligand of compound **1** is disordered over two positions with occupancy of 0.5. Similarly N3 is also disordered over two positions. Only a few H atoms could be located in the difference Fourier maps in each structure. The rest were placed in calculated positions using idealized geometries (riding model) and assigned fixed isotropic displacement parameters. Several DFIX commands were used to fix the bond distances of lattice DMF molecules. See Tables 2 and 3 for crystal and structure data for **1**, **2**, **3**, **4**, **2'**, **2a**, **2b**, and **2c**.

Acknowledgment. We gratefully acknowledge the financial support received from the DST, India (Grant No. SR/S5/GC-04/2008 to P.K.B.) and a SRF (from the CSIR) to M.K.S. We thank Profs. V. Pedireddi and J. A. R. Navarro for PXRD measurements.

Supporting Information Available: X-ray crystallographic files in CIF format for **1–4**, **2a**, **2b**, **2c**, and **2'**, IR spectra, ¹H NMR spectra, ESI mass spectra, XRPD, thermogravimetric analyses, additional figures and tables. This material is available free of charge via the Internet at <http://pubs.acs.org>.

(18) SAINT+, version 6.02; Bruker AXS: Madison, WI, 1999.

(19) Sheldrick, G. M. *SADABS, Empirical Absorption Correction Program*; University of Göttingen: Germany, 1997.

(20) XPREP, version 5.1; Siemens Industrial Automation Inc.: Madison, WI, 1995.

(21) Sheldrick, G. M. *SHELXTL Reference Manual*, version 5.1; Bruker AXS: Madison, WI, 1997.

(22) Sheldrick, G. M. *SHELXL-97, Program for Crystal Structure Refinement*; University of Göttingen: Göttingen, Germany, 1997.